國立台灣大學生命科學院生化科學研究所

碩士論文

Institute of Biochemical Sciences
College of Life Science
National Taiwan University
Master Thesis

鑑定抑制 MDA-MB-231 遷移與侵襲能力之分子標的

Identification of cellular targets for inhibiting MDA-MB-231 migration and invasion

楊明憲

Ming-Xian Yang

指導教授：梁博煌 博士

Advisor: Po-Huang Liang, Ph.D.

中華民國 108 年 6 月

June 2019

doi:10.6342/NTU201901077

國立臺灣大學碩士學位論文
口試委員會審定書

鑑定抑制 MDA-MB-231 遷移與侵襲能力之分子標的

Identification of cellular targets for inhibiting MDA-MB-231 migration and invasion

本論文係楊明憲君（學號 R06B46015）在國立臺灣大學生化科學研究所完成之碩士學位論文，於民國 108 年 6 月 6 日承下列考試委員審查通過及口試及格，特此證明。

口試委員：

林源峰 （簽名）

梁博煥　　黃世旗

（指導教授）

doi:10.6342/NTU201901077

致謝

一言著實難以道盡一路上大家的幫助與敝人感激之情。得之於人者太多，出之於己者太少。因為需要感謝的人太多了，就感謝天吧。

楊明憲 謹誌於

台灣大學生化科學研究所

中華民國 一百零八年六月

doi:10.6342/NTU201901077

Table of contents

doi:10.6342/NTU201901077

doi:10.6342/NTU201901077

doi:10.6342/NTU201901077

List of tables

doi:10.6342/NTU201901077

List of figures

doi:10.6342/NTU201901077

中文摘要

癌症轉移在腫瘤發展的過程中是個難以治療與預測的現象，現有療法仍無法有效防止癌症轉移。目前對於抑制癌症轉移的標靶性療法仍有所不足。我們研究團隊先前發現一個擁有 iodoacetamide 基團的共價抑制劑 I-Trp 能夠對 β-tubulin 354 號位置的半胱胺酸進行烷基化，因此破壞 β-tubulin 和 CCT-β 間的交互作用，更進一步誘導 CCT-β 過度表現的癌細胞進行細胞凋亡，其中包含一株三陰性乳癌細胞株 MDA-MB-231，而此株乳癌細胞株於本研究中用於測試 I-Trp 對其轉移能力之影響。本研究發現，低於半抑制濃度的 I-Trp 便能抑制 MDA-MB-231 細胞遷移和侵襲能力約 7 至 8 成。為了找出 I-Trp 於癌細胞中影響轉移能力的分子標的，本研究中利用帶有螢光基團的 I-Trp 探針，標記細胞中 I-Trp 的標靶蛋白質，再表現與癌細胞轉移有關的蛋白質進行烷基化位點研究。實驗發現被標記的其中一個蛋白為 Rab5c，而 Rab5c 於先前報導顯示有調控癌細胞移動的能力。接著，將 Rab5c 的半胱胺酸位點進行突變，並表現於 MDA-MB-231 乳癌細胞中，測試 I-Trp 對其抑制遷徙和侵襲能力。實驗發現，Rab5c 20 號以及 64 號位置的半胱胺酸會被 I-Trp 所烷基化，此外，若將這兩個位置的半胱胺酸突變為絲胺酸時，I-Trp 便會失去抑制 MDA-MB-231 細胞遷徙和侵襲能力的藥效。總結而論，Rab5c 以及先前研究發現的 β-tubulin 是 I-Trp 於細胞中的分子標的，而前者遭 I-Trp 所標的會影響癌症轉移能力，後者遭 I-Trp 標的則會誘導癌細胞凋亡。

關鍵詞：癌症轉移、小分子抑制劑、分子標的鑑定、Rab5c、細胞遷移、細胞侵襲。

doi:10.6342/NTU201901077

Abstract

Metastasis is a formidable process during tumor progression, often leading existing therapies to failure. As a result, there has been an unmet need for targeted therapies to effectively inhibit cancer metastasis. An iodoacetamide-based covalent inhibitor, I-Trp, was previously demonstrated to be capable of alkylating Cys354 of β-tubulin to disrupt the protein-protein interaction between β-tubulin and CCT-β, thus inducing apoptosis of CCT-β overexpressed cancer cells, including MDA-MB-231, a TNBC, which was used to test I-Trp on inhibiting its metastasis. In this study, a sub-IC_{50} concentration of I-Trp was found to decrease the migration and invasion of MDA-MB-231 by 70-80%. To identify the potential target for I-Trp inhibiting cell migration and invasion, total cellular proteins were treated with an I-Trp-derived fluorescent probe. The proteins labeled by I-Trp were further expressed in MDA-MB-231 to study their alkylating sites of I-Trp. One of the proteins, Rab5c, which has been reported to involve in metastasis, was mutated at the alkylating sites and transfected into MDA-MB-231 to test its role in I-Trp inhibiting cell migration and invasion. Cys20 and Cys64 of Rab5c were found to be alkylated by I-Trp and the alkylation resulted in suppression of MDA-MB-231 migration and invasion. In conclusion, this study combined with our previous findings show that I-Trp targets β-tubulin and Rab5c, thereby inducing cancer cell apoptosis and inhibiting cancer cell migration and invasion.

Keywords: cancer metastasis, small molecule inhibitor, target identification, Rab5c, cell migration, cell invasion.

doi:10.6342/NTU201901077

1. Introduction

1.1 Cancer metastasis: reasons and facts

Cancer is the leading cause of death worldwide, accounting for 9.6 million deaths in 2018 alone[1]. While cancer can be deadly, the rates of survival have decreased due to advances in screening, early detection and treatment. Regardless of much progress in medicine, during tumor progression, dissemination of primary tumor cells is still a formidable process, called metastasis, often leading existing therapies to failure. Metastasis is the onset of the spread of tumor cells away from where these tumor cells originally form. Cancer could not only spread regionally, such as nearby lymph nodes, tissues or organs, but spread to distant parts of the body. Patients diagnosed with metastatic cancer tend to have poor prognosis and survival rates partially owing to the lack of therapeutics that can efficiently block the metastatic process. For example, lung cancer that has spread to a distant organ has a 5-year survival rate of only 3%, which has not changed over the past few decades[2]. Therefore, there has been an unmet need for therapies to cure patients that are suffering from metastatic cancers.

1.2 Chemotherapy and targeted therapies: pros and cons

Currently, the usage of conventional and available chemotherapies often fails to prevent cancer recurrence since these therapies cannot completely eliminate cancer cells

doi:10.6342/NTU201901077

and these remaining cancer cells would gradually disseminate throughout the body. Furthermore, most chemotherapies would cause many severe adverse effects, including gastrointestinal distress[3], hair loss[4,5] or even infertility[6]. In these regards, targeted therapy has been put lots of efforts and has become a promising alternative in clinical medicine, which shows less toxicity and better tolerance in the human body. Targeted therapy is one of major treatments of cancers, which blocks the growth of cancer cells by interfering with specific molecular targets required for tumorigenesis and tumor growth instead of simply suppressing rapid cell proliferation like cytotoxic chemotherapy.

1.3 Target identification

There are several approaches to discovering protein targets of a small molecule. Most of approaches fall into three main categories: direct biochemical methods, genetic interaction methods and computational inference methods. Direct biochemical methods take advantages of matrix-based detection or matrix-free affinity labeling for target identification. Matrix-based detection fuses a small molecule of interest to a solid support or capturable moiety like biotin in order that proteins targeted by the small molecule could be enriched[7,8]. Matrix-free affinity labeling relies on the incorporation of radioisotope, photo-reactive or fluorescent labels into a small molecule of interest. Despite convenience of direct biochemical methods, it is of particular importance that the bioactivity/binding

doi:10.6342/NTU201901077

specificity of the small molecule should not be compromised by the derivatization. Genetic interaction methods leverage the ease of working with DNA and RNA to perform large scale modifications and measurements. These methods rely on the idea of genetic modifiers, such as enhancers or suppressors, to generate targets hypotheses[9]. However, genetic perturbations cannot always recapitulate the effect of a small molecule due to the risk of genetic compensation. Computational methods are used to infer potential protein targets of small molecules or even to find new targets of the existing drugs with the goal of drug repurposing or explaining off-target effects[10,11]. Theoretically, inference-based methods are the least bias of any target identification methods because they often rely on experiments done by others. In this study, fluorescent labeling was employed to identify potential targets of I-Trp for inhibiting MDA-MB-231 migration and invasion.

1.4 Rab5c: a player in focal adhesion disassembly and the link with tumor cell migration and invasion

The small GTPase Rab5 is a critical regulator of vesicle and early endosome dynamics[12], however, it has also been reported to be implicated in cell migration. Rab5 associates with β1 integrins, a component of focal adhesion, leading to their internalization. Except for β1 integrin, Rab5 was also found to be associated with other focal adhesion molecules, including Vinculin, Paxillin and Focal adhesion kinase (FAK)[13].

doi:10.6342/NTU201901077

Focal adhesion is a complex formed by more than 150 different proteins like kinases, adaptor and scaffold proteins as well as actin linking proteins. Formation of these complexes sustains cellular contact with the extracellular matrix and regulation of these interactions and dynamics of focal adhesions are crucial for cell directional migration[14]. Rab5 can promote focal adhesion disassembly in tumor cells, thus stimulating cellular protrusions and sustaining tumor cell migration and invasion[13] (Fig 1).

1.5 Previous and the present studies

According to our previous studies, an iodoacetamide-based covalent inhibitor, I-Trp (Fig. 2A), was proven to be capable of alkylating Cys354 of β-tubulin and thus disrupting the protein-protein interaction between β-tubulin and CCT-β[15]. By targeting β-tubulin, I-Trp can induce ER-stress, caspases activation and cause apoptosis of CCT-β overexpressed cancer cells[16,17], such as MDA-MB-231, a highly metastatic TNBC, which was used to test I-Trp on inhibiting its metastasis. However, the efficacy of I-Trp against cancer metastasis remains unknown. In addition, whether other cellular targets play some roles in I-Trp inhibiting cell migration and invasion need to be investigated. In this study, we provide evidence for Rab5c, a protein mediating early endosomal trafficking, as a target of I-Trp. The alkylation of Rab5c at Cys residues impairs focal adhesion assembly/disassembly dynamics, thereby leading to suppression of MDA-MB-231

doi:10.6342/NTU201901077

migration and invasion.

doi:10.6342/NTU201901077

2. Materials and methods

2.1 Cell culture

MDA-MB-231 cell line was purchased from Bio-resource Collection and Research Center (Hsinchu, Taiwan). HEK-293T was a gift from Dr. Shih-Hsiung Wu (Institute of Biological chemistry, Academia Sinica). The cells were cultured in Dulbecco's modified Eagle's medium supplemented with 10% FBS and 1X Antibiotic-Antimycotic Solution (Corning, Manassas, VA, USA). Dulbecco's modified Eagle's medium and FBS were purchased from Gibco (Carlsbad, CA, USA). Cultures were maintained in a humidified incubator at 37℃ in the presence of 5% CO_2.

2.2 Chemicals and antibodies

I-Trp and I-Trp-Dan were synthesized as described previously[15]. To determine the levels of total, active or expressed proteins, immunoblot analyses were performed using the antibody to Rab5c (NBP1-80858, Novus Biologicals, Centennial, Colo, USA), integrin β1 (D2E5, Cell Signaling Technology, Inc., Danvers, MA, USA; GTX15769, Genetex, Hsinchu, Taiwan), β-tubulin (BT7R, Thermo Fisher Scientific Co., Fair Lawn, NJ, USA) and HA tag (GTX115044, Genetex, Hsinchu, Taiwan). The antibody recognized GAPDH (GTX100118) was purchased from Genetex (Hsinchu, Taiwan) and used to control for total protein expression.

doi:10.6342/NTU201901077

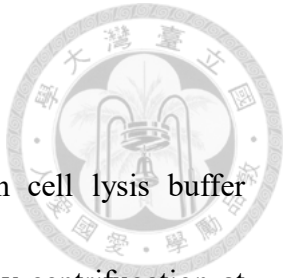

2.3 Immunoblotting

Cells were washed twice with PBS followed by lysis with cell lysis buffer (BioVision Inc., Milpitas, CA, USA). Lysates were then clarified by centrifugation at 15,000 g for 30 min at 4℃. Protein concentration was determined using Protein Assay Dye Reagent (Bio-Rad, Hercules, CA, USA). Standard immunoblotting procedures were followed. Membranes were blocked in 5% nonfat dried milk in TBS containing 0.2% Tween-20 (Cyrusbioscience, Taipei, Taiwan) and then probed with appropriate dilution of the primary antibodies and secondary antibody conjugated to horseradish peroxidase (HRP). Immuno-reactive protein bands were visualized using the enhanced chemiluminescence (ECL) system (Amersham Bioscience, Tokyo, Japan).

2.4 Wound healing assay

MDA-MB-231 cells (2.5×10^5) were seeded in a 24-well plate and incubated for 16-18 hours. The even wounds were created using a sterile 200 μl tip. The cells were then incubated for further 24 hours with Dulbecco's modified Eagle's medium in the absence or in the presence of 0.63 μM I-Trp. Images of wound area were captured using a camera attached to a light microscope (Leica, Wetzlar, Germany) and then analyzed by ImageJ software.

doi:10.6342/NTU201901077

2.5 Transwell invasion assay

Transwell invasion assay was performed using Matrigel Invasion Chambers with 8.0 μm PET Membrane (BioCoat, Horsham, PA, USA). MDA-MB-231 cells (1.0×10^5) in combination with Dulbecco's modified Eagle's medium in the absence or in the presence of 0.63 μM I-Trp were loaded into each upper chamber. The lower chamber was filled with DMEM containing 10% FBS. The whole plate was incubated for 24 hours. After 24 hours, non-invasive cells were removed using cotton swabs and cells on the bottom side of the insert were fixed with methanol for 10 min. After fixation, cells were stained with 0.2% crystal violet solution for 10 min followed by extensively washed with PBS for several times. Invasive cells were photographed using a camera attached to a light microscope and then analyzed by ImageJ software.

2.6 Mass spectrometric analysis

MDA-MB-231 cells were treated with 2 μM I-Trp-Dan at 37°C for 6 hours. The cell lysates were subjected to electrophoresis on a 10% SDS-PAGE gel. The protein bands were visualized under UV irradiation and excised from the gel. These bands were then subjected to in-gel tryptic digestion and liquid chromatography electrospray ionization-tandem mass spectrometric analysis. The raw data were converted to the Mascot (Matrix Science) generic format and used for searching against the Swiss-Prot human protein

doi:10.6342/NTU201901077

database. For peptide mass fingerprinting, recombinant proteins (30 μg) were incubated with I-Trp (molar ratio= 1:1) at 37℃ for 24 hours and the mixture was processed as described above for Mass spectrometric analysis but with some modifications. The resultant m/z values of each peptide fragment were compared with predicted molecular weight of the peptide fragment derived from human Rab5c to assess possible I-Trp-alkylated Cys residues.

2.7 Cloning of *rab5c*, *tubb* and their derivatives

All primers used in this study are shown in Table 1. Total RNA extracts from MDA-MB-231 were reverse-transcribed into cDNA using GScript First-Strand Synthesis Kit (GeneDireX, Taipei, Taiwan) which were used as the templates for the following PCR procedures. cDNA was amplified by PrimeSTAR GXL DNA Polymerase (Takara Bio USA, Inc., Mountain View, CA, USA). Site-directed mutagenesis was performed using KOD One PCR Master Mix (Toyobo, Inc., Osaka, Japan).

2.8 Expression and purification of Rab5c

The plasmid encoding *rab5c* was transformed into BL21 (DE3). The bacterial culture was grown in LB media supplemented with 50 μg/mL kanamycin at 37℃ until OD_{600} reached 0.6. The expression of Rab5c was induced with 1 mM isopropyl-β-D-

doi:10.6342/NTU201901077

thiogalactoside (IPTG) at 25℃ for overnight. The harvested bacterial cells were re-suspended in lysis buffer (50 mM Tris-HCl pH 7.4, 500 mM NaCl, 10 mM imidazole and 0.1% 2-Mercaptoethanol) for disruption. The clarified supernatant was then subjected to Ni-NTA resin (Sigma-Aldrich, Inc., St. Louis, MO, USA), washed with lysis buffer containing 20, 50, 75 mM imidazole and eluted with lysis buffer containing 250 mM imidazole. The eluent was dialyzed to the storage buffer (25 mM Tris-HCl pH 7.4, 150 mM NaCl and 0.014% 2-Mercaptoethanol). The protein aliquots were stored at -80℃.

2.9 Rab5c-GTP pulldown assay

The Rab5-binding domain (R5BD) of Rabaptin5 (a.a.739-862) was amplified from human total cDNA by PCR and ligated into pHTPP13[18]. GST-R5BD was expressed in BL21 (DE3) (Fig. 3) and purified by glutathione agarose resin (Gold Biotechnology, St. Louis, MO, USA). MDA-MB-231 cells were treated with or without 0.63 μM I-Trp, then lysed in Rab5-binding buffer (25 mM HEPES pH 7.4, 100 mM NaCl, 5 mM $MgCl_2$, 0.1% NP-40, 10% glycerol and 1 mM DTT) supplemented with 1X protease inhibitor cocktail (Roche, Basel, switzerland). 30 μg of GST-R5BD was first immobilized onto glutathione agarose resin and incubated with 1.2 mg cell lysates of each condition for overnight at 4℃, and then washed with Rab5-binding buffer for four times. The amount of active Rab5c bound to GST-R5BD was detected by immunoblotting using an anti-Rab5c

doi:10.6342/NTU201901077

antibody.

2.10 Integrin internalization assay

MDA-MB-231 cells were grown at 80% confluency on a 15-cm cell culture dish. Cells were treated either with or without 0.63 μM I-Trp for 24 hours. After 24 hours, cells were serum starved for 1 hour, transferred to ice, washed twice in cold PBS and labelled with 0.2 mg/mL Sulfo-NHS-SS-biotin (BioVision, Inc., Milpitas, CA, USA) for 30 min. Labelled cells were washed in cold PBS and transferred to Dulbecco's modified Eagle's medium with 0.6 μM primaquine (Abcam, Cambridge, UK) to allow internalization. At indicated times, the medium was removed and dishes were plated on ice. Cells were briefly washed with cold PBS twice. The biotin was removed from the proteins remaining on the cell surface by incubation with 20 mM MESNa (Abcam, Cambridge, UK) in TBS for 15 min at 4℃ and MESNa was then quenched with 20 mM iodoacetamide in TBS. Cells were lysed and subjected to capture ELISA assay to quantify the amount of internalized integrin β1.

2.11 Capture ELISA assay

Corning 96 Well Clear polystyrene High Bind Stripwell Microplate (Corning, Manassas, VA, USA) was coated with 5 μg/mL integrin β1 antibody in 0.05 M Na_2CO_3 (pH 9.6) at 4℃ overnight. After overnight coating, the microplate was washed for three

doi:10.6342/NTU201901077

times with PBST (0.05% Tween-20) for 5 min and blocked with PBST containing 5% BSA for 1 hour. Integrin β1 was captured by overnight incubation of appropriate amount of cell lysates at 4℃. Unbound materials were removed by extensive wash with PBST. The captured integrin β1 was probed by streptavidin-conjugated horseradish peroxidase (GTX85912, Genetex, Hsinchu, Taiwan) in PBST containing 1% BSA. Biotinylated integrin β1 was detected by a chromogenic reaction with TMB solution (BioVision, Inc., Milpitas, CA, USA).

2.12 Production of cDNA-expressing viruses

Each cDNA-expressing virus was prepared by co-transfection of the cDNA of interest which was cloned into pLAS3w_puro vector, pCMV-Δ8.91, and pMD.G plasmids into HEK293t using TurboFect transfection reagent (Thermo Fisher Scientific Co., Fair Lawn, NJ, USA) according to the procedure provided by National RNAi Core Facility (Academia Sinica, Taiwan). Cultures of virus-infected MDA-MB-231 cells were continuously selected with 2 μg/mL puromycin (Gold Biotechnology, St. Louis, MO, USA).

2.13 Statistical analysis

Data were shown as mean with standard deviation (SD). The statistical difference

doi:10.6342/NTU201901077

was evaluated by the Student's t-test for normal distributed values and by non-parametric Mann-Whitney t-test for values of non-normal distribution. Survival durations of patients were analyzed by Kaplan–Meier method and compared using the log-rank test in the patient groups. Values of $p < 0.05$ were considered significant.

doi:10.6342/NTU201901077

3. Results

3.1 I-Trp inhibited MDA-MB-231 migration and invasion

It has been reported in the previous study[17] that CCT-β-overexpressed cancer cell lines were more susceptible to I-Trp. Therefore, in this study, one of the CCT-β-overexpressed cancer cell line, MDA-MD-231, was used to test whether I-Trp can inhibit its migration and invasion. To test the efficacy of I-Trp against MDA-MB-231 migration *in-vitro*, wound healing assay was performed for 24 hours (Fig. 4). Treatment of I-Trp resulted in a dose-dependent inhibition of cell migration after 24 hours. The maximal inhibition (~70%) of I-Trp was observed when a sub-IC_{50} concentration of I-Trp (IC_{50} = 1.28 μM; Fig. 2B) was administered. Apart from cell migration, cell invasions is also a major characteristic of cancer metastasis[19]. MDA-MB-231 cell invasiveness was assessed by transwell invasion assay using Matrigel Invasion Chambers with 8.0 μm pores on the PET Membrane (Fig. 5). As shown in Figure 5, treatment of I-Trp led to remarkable decrease in MDA-MB-231 invasion by up to 80%. Together, these results indicated that I-Trp exerted potent efficacy against MDA-MB-231 migration and invasion.

3.2 Identification of the potential target of I-Trp for inhibiting MDA-MB-231 migration and invasion

I-Trp was demonstrated above to be capable of inhibiting MDA-MB-231 migration

doi:10.6342/NTU201901077

and invasion. We next sought to explore potential cellular targets of I-Trp that contribute to the inhibitory efficacy of I-Trp. Based on the approach used in the previous study[15], I-Trp-derived fluorescent probe, I-Trp-Dan (IC_{50}= 2.13 μM; Fig. 6A, B) with the potency similar to I-Trp, was used to label cellular targets of I-Trp. After treatment of I-Trp-Dan for 6 hours, MDA-MB-231 cells were lysed and the cell lysate was subjected to SDS-PAGE. When electrophoresis was performed using glycine buffer system, a clear fluorescent band was found to locate around 50 kDa (Fig. 6C, *left*), revealing the previously identified cellular target, β-tubulin. However, while electrophoresis was performed using tricine buffer system, multiple protein bands were resolved, suggesting that cellular targets of I-Trp other than β-tubulin could exist and these targets may play some roles in the inhibitory effect of I-Trp. To identify the cellular targets for inhibiting MDA-MB-231 migration and invasion, the visualized protein bands (Fig. 6C, *right*; band A, B and C) were excised from the gel and subjected to mass spectrometric analysis. As expected, β-tubulin was identified in band B which showed the matched molecular weight. After ruling out the identified proteins not reported to be involved in cancer cell motility or metastasis, Rab5c was possibly the target for the inhibitory effect of I-Trp on MDA-MB-231 migration and invasion since it has been reported that Rab5c plays a pivotal role in mediating focal adhesion assembly/ disassembly dynamics, cancer cell motility, cancer invasion and metastasis[13,20-22].

doi:10.6342/NTU201901077

3.3 I-Trp suppressed Rab5c activity and Rab5c-mediated integrin β1 internalization

Given that Rab5c was identified to be a potential target of I-Trp, the activity of Rab5c might be suppressed after I-Trp treatment. To investigate whether the activity of Rab5c is affected after I-Trp treatment, the amount of active Rab5c (GTP-bound Rab5c) was evaluated using Rab5c-GTP pull-down assay. As anticipated, active Rab5c level significantly decreased after I-Trp treatment for 24 hours and this effect was not due to the decrease in the total protein level of Rab5c (Fig. 7A). Moreover, since Rab5c was reported to be implicated in integrin internalization, a process of focal adhesion dynamics[22,23], we hypothesized that the rates of integrin internalization might be affected upon I-Trp treatment. To this end, MDA-MB-231 cells were pre-treated with 0.63 μM I-Trp for 24 hours followed by integrin internalization assay. Dynamic studies of surface integrin β1 internalization revealed slower rates of internalization among cells treated with I-Trp (Fig 7C). However, the overall capacity of cells treated with I-Trp, given enough time (15 min), was similar to those treated without I-Trp. These results indicated that Rab5c activity and its relevant effects were suppressed by I-Trp.

3.4 Determination of alkylating sites of I-Trp in Rab5c

Next, to identify the exact alkylating sites of I-Trp in Rab5c, purified human recombinant Rab5c (Fig. 8) was incubated with I-Trp at the molar ratio of 1:1 at 37°C for

doi:10.6342/NTU201901077

24 hours. The mixture was then subjected to SDS-PAGE followed by in gel tryptic digestion and the peptides were analyzed by MS/MS. The peptide mass fingerprinting analysis revealed that peptides with monoisotopic masses were consistent with Cys20 and Cys64 incorporated with N-acetyl-Trp group (Fig. 9A and B). Interestingly, human Rab5c contains four cysteine residues, Cys20, Cys64, Cys213 and Cys214, yet peptides containing Cys213 and Cys214 formed no adducts with I-Trp, suggesting the selective alkylation of Cys20 and Cys64 by I-Trp. Furthermore, the model processed by the molecular docking showed that the Cys20 and Cys64 were far away from the active site (Fig. 10), indicating the inhibitory effect of I-Trp was probably not due to the competition with the ligand binding (GTP-Mg^{2+}). The above findings suggested that Cys20 and Cys64 of Rab5c could be simultaneously alkylated by I-Trp and the alkylation step might be pivotal for the inhibitory effect of I-Trp on MDA-MB-231 migration and invasion.

3.5 Validation of alkylating sites of I-Trp in Rab5c in MDA-MB-231

To validate whether the inhibitory effect of I-Trp was due to alkylation at the cysteine residues, C20S and C64S Rab5c were respectively expressed in MDA-MB-231. Apart from Rab5c, Cys354 of β-tubulin is also a target of I-Trp[15]. Thus, C354S β-tubulin was also expressed in MDA-MB-231 to test whether this alkylation could play some roles in I-Trp inhibiting MDA-MB-231 migration and invasion. From wound healing assays, the

doi:10.6342/NTU201901077

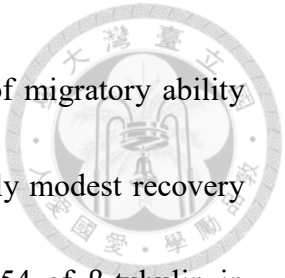

expression of either C20S or C64S gave rise to 25~30% recovery of migratory ability (Fig. 11A), whereas the expression of Cys354 β-tubulin showed only modest recovery (Fig. 11B), thus indicating the specific role of alkylation of Cys354 of β-tubulin in apoptosis rather than inhibition of migration and invasion upon I-Trp treatment. Next, we set out to express double mutants of Rab5c (C20S/C64S) to investigate whether migration of MDA-MB-231 with this mutant Rab5c (C20S/C64S) could resuscitate to the original state. Meanwhile, C354S β-tubulin in combination of double mutants of Rab5c were also expressed in MDA-MB-231 to examine if C354S β-tubulin could further contribute to the recovery effect. As anticipated, without C354S β-tubulin, the expression of double mutants of Rab5c (C20S/C64S) was shown to be enough to result in full recovery of MDA-MB-231 migration (Fig. 11C). The expression of both C354S β-tubulin and double mutants of Rabc5c (C20S/C64S) displayed the similar effect to the expression of double mutants of Rab5c. These results suggested that I-Trp targets Rab5c by alkylating both Cys20 and Cys64 to exert the inhibitory effect on MDA-MB-231 migration.

doi:10.6342/NTU201901077

4. Discussion

The efficacy of most of current anti-cancer agents depends on the capability of causing genotoxicity or cytotoxicity. Nevertheless, cancer cells often obtain the ability to circumvent the death programs induced by the agents and thus resulted in recurrence or clinically detectable metastasis[24]. Metastasis is responsible for the cancer-relevant mortality and still remains a major challenge in current cancer therapies. This situation promotes the development of more specific therapeutics targeting cancer metastasis. In the present study, I-Trp is demonstrated to possess the potency against cancer cell migration and invasion.

It is noteworthy that the importance of endosome trafficking and membrane dynamics in metastasis has been well elucidated. Endocytosis is involved in various cellular processes, including uptake and internalization of extracellular molecules[25], regulation of signaling induced by extracellular ligands[26], trafficking of surface receptors[27] and rearrangement of cytoskeleton[28]. Endocytosis and intracellular trafficking are coordinated by a family of small GTPases called Rabs. Among Rab proteins, Rab5 is one of the best characterized, mediating various cellular functions like vesicle formation[29], early endosome fusion[30] and motility along microtubules[31]. Furthermore, previous studies have suggested important roles of Rab5 in focal adhesion disassembly, migration and invasiveness in tumor cells[13,21,32]. It is also of particular importance that high expression

doi:10.6342/NTU201901077

of Rab5c correlated with poor patient survival (Fig. 12). Though our previous study reported that I-Trp targets β-tubulin, alkylates Cys354 of β-tubulin and thus induces cancer cell apoptosis, targeting Cys354 of β-tubulin cannot endow I-Trp with the inhibitory effect on MDA-MB-231 migration (Fig. 11B), indicating that other cellular proteins targeted by I-Trp might be involved in this effect. Using peptide mass fingerprinting analysis, the present work revealed that Rab5c in MDA-MB-231 was targeted and alkylated by I-Trp at Cys20 and Cys64. As a result, the function of Rab5c was impaired and integrin β1 trafficking was delayed (Fig. 7A-C), again suggesting that the aberrant endocytosis leads to loss of metastatic capability of cancer cells. However, the *in vivo* efficacy of I-Trp against cancer metastasis remains to be investigated.

There has been considerable debate over the role of Rab5 isoforms in cancer metastasis. Some have suggested that Rab5a is the critical mediator of cancer cell motility and invasiveness[13,33], whereas others have argued that Rab5c plays the preferential role in cancer cell migration and invasion[20,21]. Among our findings, Rab5c was identified to be targeted by I-Trp in MDA-MB-231, which is in accordance with the validation experiments (Fig. 11A-C); however, these findings cannot exclude the importance of Rab5a in cancer metastasis.

To sum up, our work demonstrates that I-Trp regulates metastatic-related biological processes closely linked to Rab5c and further identifies that Rab5c is a cellular target for

doi:10.6342/NTU201901077

I-Trp inhibiting MDA-MB-231 migration and invasion and also Cys20 and Cys64 of Rab5c are the alkylating sites of I-Trp, thus raising the notion that Rab5c could be a molecular target for the development of therapeutic agents aimed at inhibiting cancer metastasis.

doi:10.6342/NTU201901077

Tables

Table 1. Primers used in this study

Primer	Sequence (5'-3')	Cloning
rab5c forward	ATCGAGAGCTCATGGCGGGTCGGGG	SacI
rab5c reverse	ATCGACTCGAGTTAGTTGCTGCAGCACTG	XhoI
rab5c forward (lentivirus)	ATCGAGCTAGCACCATGGCGGGTCGGGG	NheI
rab5c reverse (lentivirus)	ATCGACCTGCAGGTTAGTTGCTGCAGCACTG	SbfI
rabaptin (a.a.739-862) forward	ATCGAGAATTCGCTTCTATTTCTAGCCTAAAAG	EcoRI
rabaptin (a.a.739-862) reverse	ATCGACTCGAGTTATGTCTCAGGAAGCTGG	XhoI
tubb forward	ATCGAGCTAGCACCATGAGGGAAATCGTGCACTTG	NheI
tubb-HA reverse	ATCGAGAATTCCTAAGCGTAATCTGGAACATCGTATGGGTAGGCCACCTCCTCCTCAG	EcoRI

doi:10.6342/NTU201901077

rab5c C20S forward	GCTGCTGGGAACAAGATCAGTC AATTTAAGCTGGTTC	Site-directed mutagenesis
rab5c C20S reverse	GAACCAGCTTAAATTGACTGATC TTGTTCCCAGCAGC	Site-directed mutagenesis
rab5c C64S forward	CCTCACACAGACTGTCAGCCTGG ATGACACAAC	Site-directed mutagenesis
rab5c C64S reverse	GTTGTGTCATCCAGGCTGACAGT CTGTGTGAGG	Site-directed mutagenesis
tubb C354S forward	GTGAAAACGGCTGTCAGTGACAT CCCACCTC	Site-directed mutagenesis
tubb C354S reverse	GAGGTGGGATGTCACTGACAGC CGTTTTCAC	Site-directed mutagenesis
C20S/C64S *rab5c*-2A forward	CCCAAGCTGGCTAGC	Co-expression of Rab5c and β-tubulin
C20S/C64S *rab5c*-2A reverse	GTCTCCAGCCTGCTTCAGCAGGC TGAAGTTAGTAGCTCCGCTTCCG TTGCTGCAGCACTG	Co-expression of Rab5c and β-tubulin
2A- C354S *tubb* forward	GCTACTAACTTCAGCCTGCTGAA GCAGGCTGGAGACGTGGAGGAG AACCCTGGACCTATGAGGGAAAT CGTGC	Co-expression of Rab5c and β-tubulin

doi:10.6342/NTU201901077

2A- C354S *tubb* reverse	CAAGATCTAGAATTCCTAAGCG	Co-expression of Rab5c and β-tubulin

doi:10.6342/NTU201901077

Table 2. Identification of cellular targets by mass spectrometric analysis

UniprotID	Protein names	Functions	Molecular weight (kDa)	Band
P10809	60 kDa heat shock protein, mitochondrial	chaperone	61.2	A
P14618	Pyruvate kinase PKM	glycolysis	58.5	A
P07237	Protein disulfide-isomerase	chaperone	57.5	A
P17987	T-complex protein 1 subunit alpha	chaperone	60.8	A
P49368	T-complex protein 1 subunit gamma	chaperone	61.1	A
P06733	Alpha-enolase	glycolysis	47.5	B
P06576	ATP synthase subunit beta, mitochondrial	oxidative phosphorylation	56.5	B
Q13885	Tubulin beta-2A chain	cytoskeletal protein	50.3	B
Q9BQE3	Tubulin alpha-1C chain	cytoskeletal protein	50.5	B
P50395	Rab GDP dissociation inhibitor beta	GDP/GTP exchange	51.1	B
P09211	Glutathione S-transferase P	detoxification	23.6	C

doi:10.6342/NTU201901077

P04406	Glyceraldehyde-3-phosphate dehydrogenase	glycolysis	36.2	C
P51148	Ras-related protein Rab-5C	endosomal vesicles trafficking	23.7	C
P28070	Proteasome subunit beta type-4	proteolytic degradation	29.2	C

doi:10.6342/NTU201901077

Figures

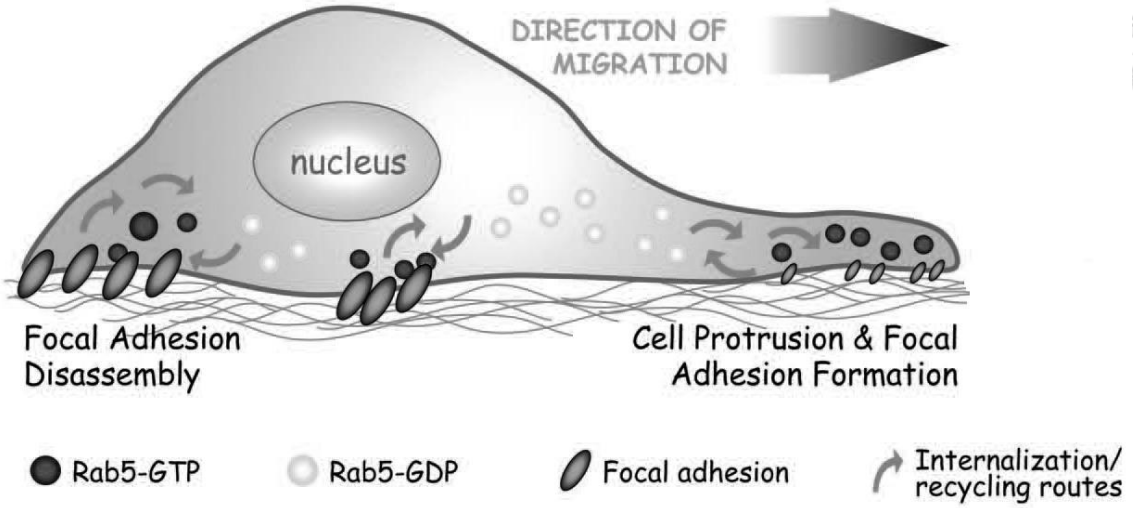

Figure 1. The scheme shows Rab5-driven cell migration and invasion. Rab5 promotes focal adhesions disassembly, leading to sustained and directional cell migration. Adapted from "Rab'ing tumor cell migration and invasion: focal adhesion disassembly driven by Rab5," by Torres, V. A., 2014, *Cell adhesion & migration, 8*, P. 86. Copyright 2014 by Taylor & Francis group.

doi:10.6342/NTU201901077

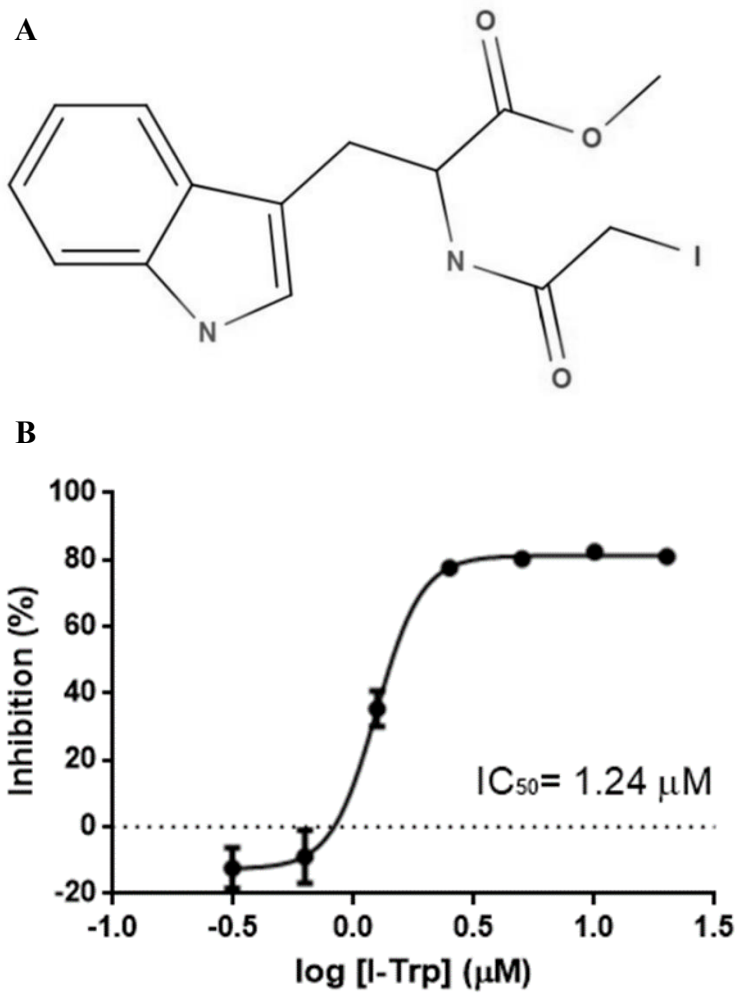

Figure 2. The chemical structure of I-Trp and MTT assay evaluating I-Trp efficacy. (A) The chemical structure of I-Trp. (B) The IC_{50} of I-Trp against MDA-MB-231 was 1.24 μM. Cells were treated with I-Trp for 24 hours.

doi:10.6342/NTU201901077

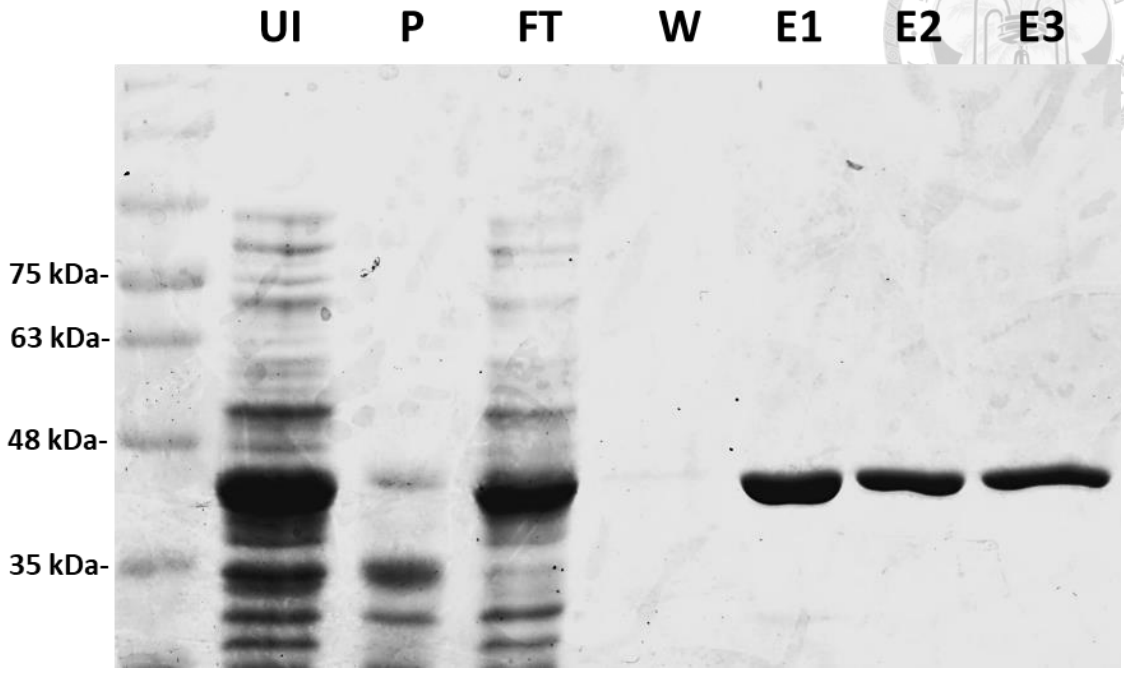

Figure 3. Purified Rabaptin5 (a.a.739-862; Rab5-binding domain, R5BD) was analyzed by SDS-PAGE. UI: cell lysate from the cell un-induced with 1 mM IPTG, P: insoluble fraction after cell disruption, FT: flow through after soluble fraction binding to glutathione agarose beads, W: washed with PBS, E1, E2, E3: eluted with the buffer containing 50 mM Tris pH 6.0 and 10 mM glutathione.

doi:10.6342/NTU201901077

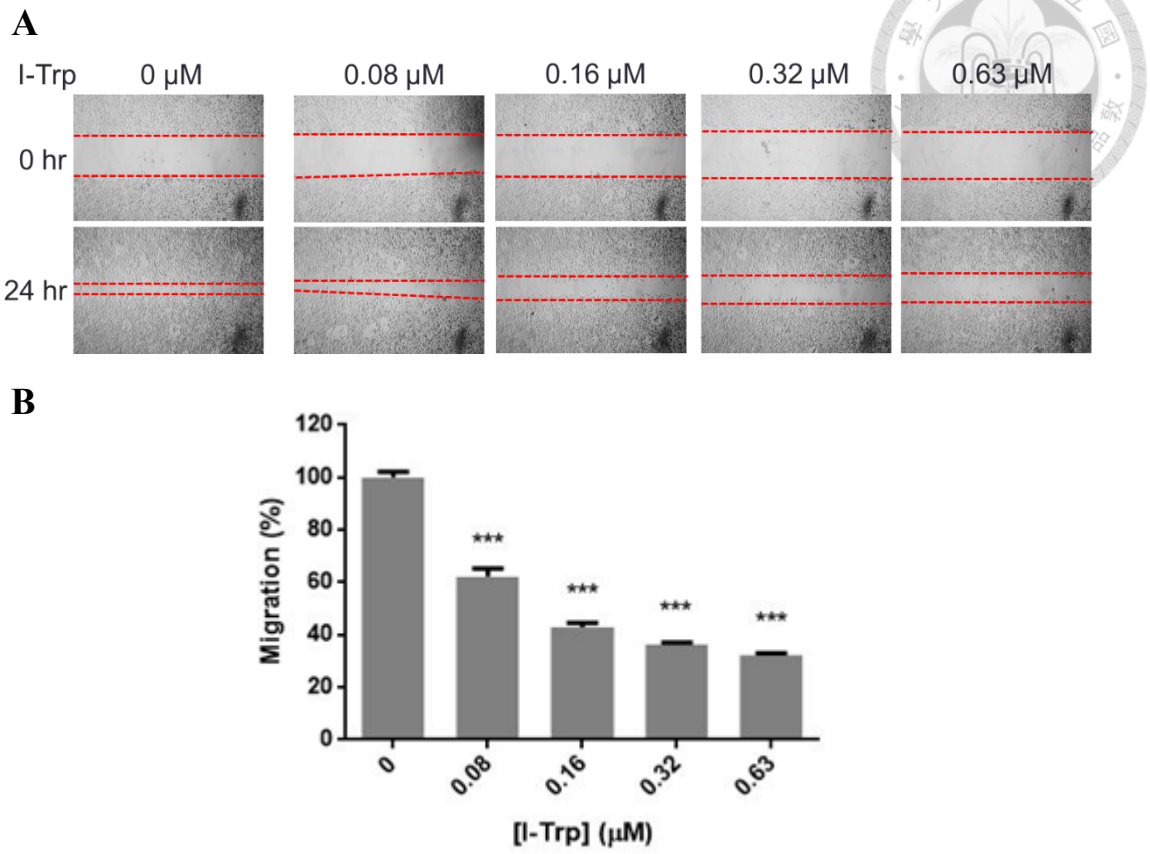

Figure 4. I-Trp inhibited MDA-MB-231 migration in a dose-dependent manner after 24-hour treatment. (A) Representative images of wound healing assays. (B) Graphical representation of percentage of cell migration. Statistical testing was performed by using the unpaired two-sided Student's *t* test; ***P<0.001 versus untreated group.

doi:10.6342/NTU201901077

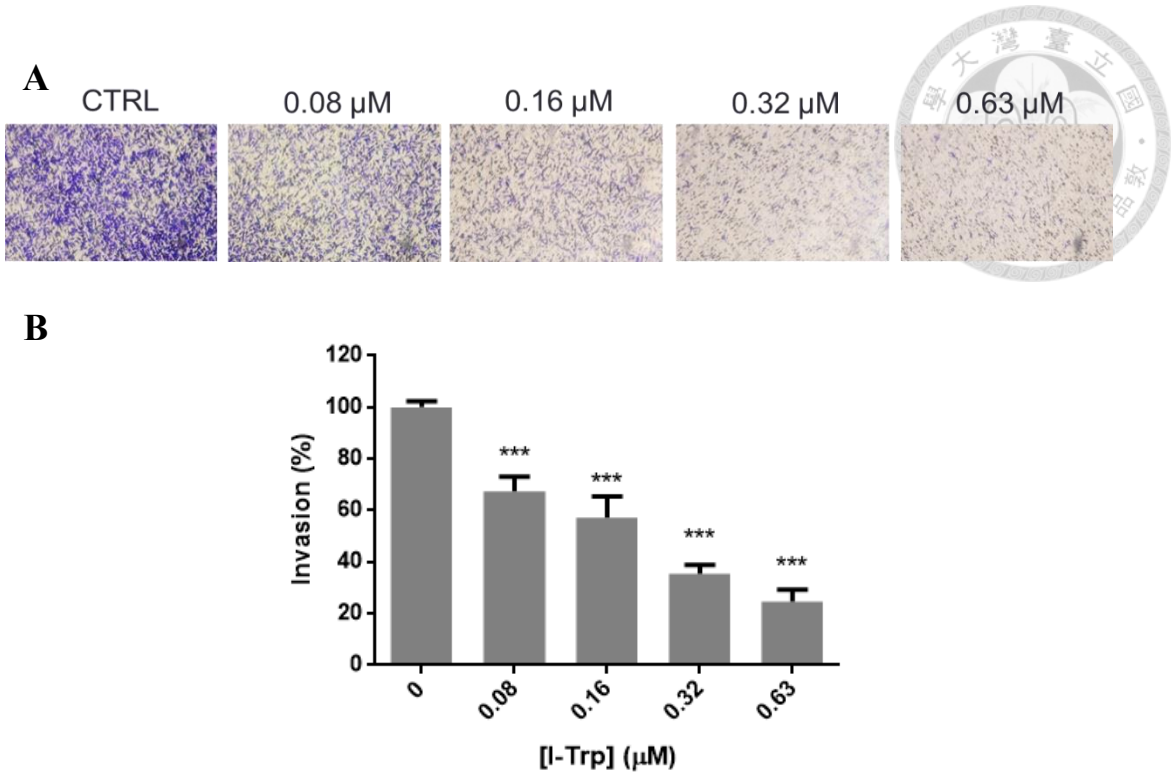

Figure 5. I-Trp inhibited MDA-MB-231 invasion in a dose-dependent manner after 24-hour treatment. (A) Representative images of transwell assays. (B) Graphical representation of percent cell invasion. Statistical testing was performed by using the unpaired two-sided Student's *t* test; ***P<0.001 versus untreated group.

doi:10.6342/NTU201901077

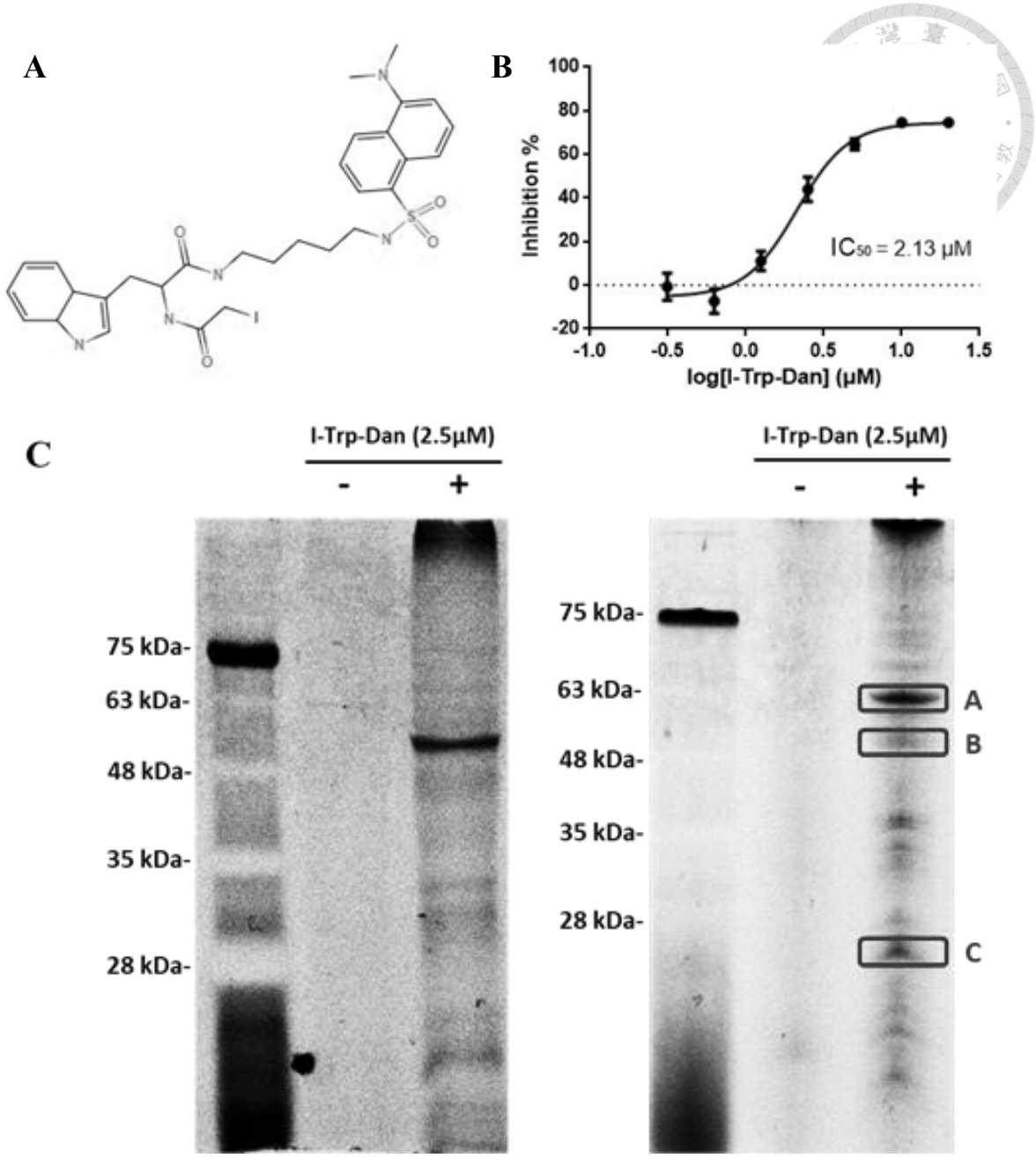

Figure 6. Identification of cellular targets of I-Trp using I-Trp-derived fluorescent probe, I-Trp-Dan. (A) The chemical structure of I-Trp-Dan. (B) I-Trp-Dan showed inhibitory effect against MDA-MB-231 with an IC_{50} of 2.13 μM. (C) Cells were treated with or without 2.5 μM I-Trp-Dan for 6 hours and cell lysates were subjected to SDS-PAGE run with either glycine (*left*) or tricine (*right*) buffer system. The labeled protein bands were visualized under UV irradiation and the images were processed inverted.

doi:10.6342/NTU201901077

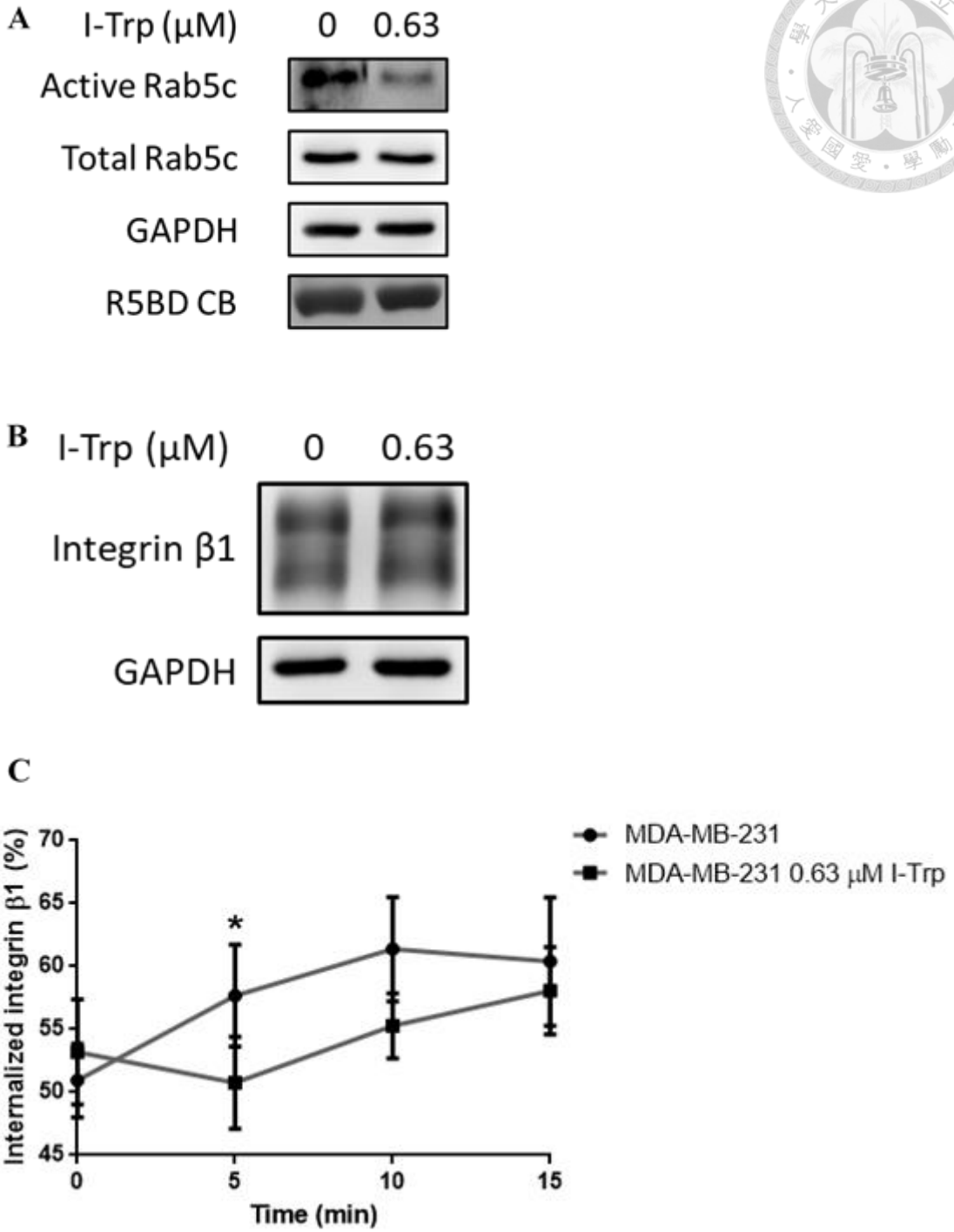

Figure 7. I-Trp suppressed Rab5c activity and Rab5c-mediated integrin β1 internalization. (A) Total Rab5c remained unchanged but active Rab5c was decreased after I-Trp treatment for 24 hours. (B) I-Trp treatment did not affect total level of integrin β1. (C) Internalization of integrin β1 was delayed when MDA-MB-231 was treated with 0.63 μM I-Trp. Statistical testing was performed by using the unpaired two-sided Student's *t* test; **P*<0.05 versus untreated group.

doi:10.6342/NTU201901077

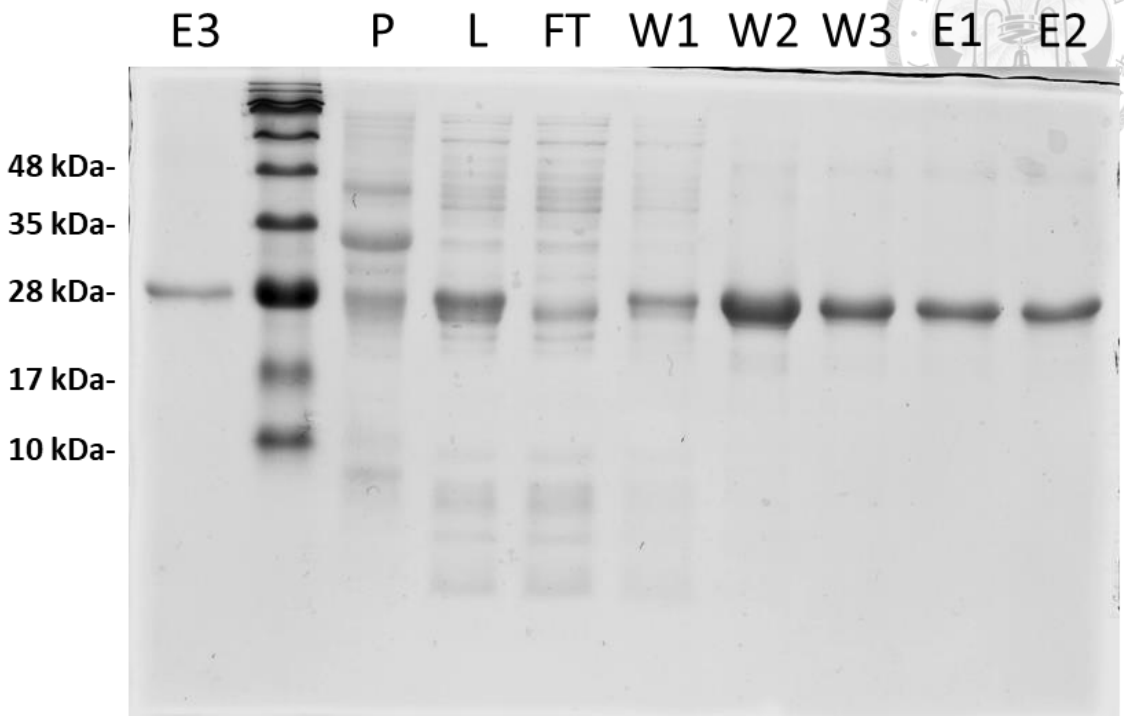

Figure 8. Purified Rab5c was analyzed by SDS-PAGE. P: insoluble fraction after cell disruption, L: soluble fraction, FT: flow through after soluble fraction binding to Ni-NTA, W1: washed with binding buffer containing 20 mM imidazole, W2: washed with binding buffer containing 50 mM imidazole, W3: washed with binding buffer containing 75 mM imidazole, E1, E2, E3: eluted fractions with binding buffer containing 250 mM imidazole.

doi:10.6342/NTU201901077

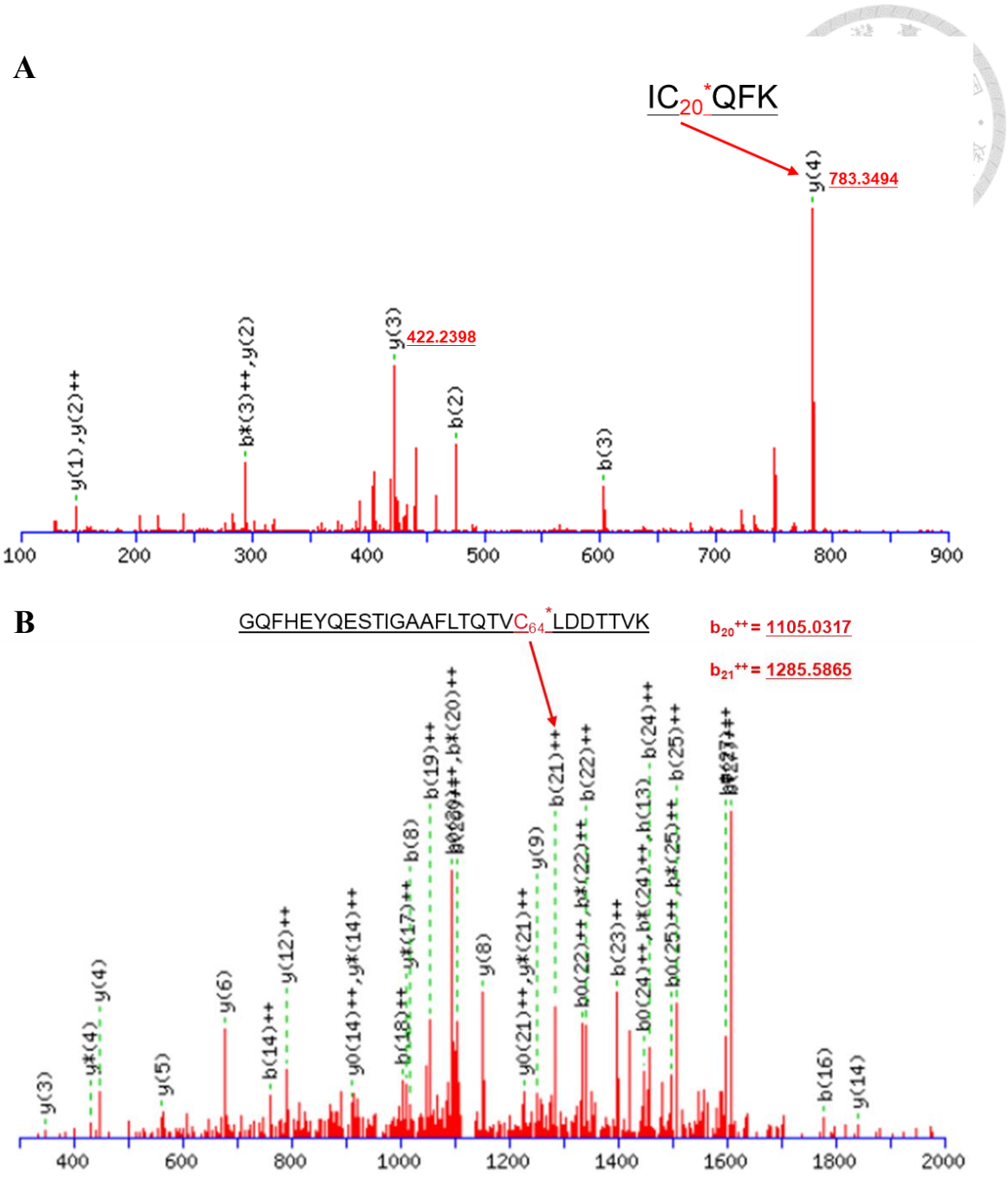

Figure 9. Representative MS_2 spectra showing alkylated peptides by I-Trp. The peptides with I-Trp alkylation showed a shift in monoisotopic mass of +258 Da**.** (A) The peptide containing Cys20 was alkylated by I-Trp. (B) The peptide containing Cys64 was alkylated by I-Trp.

doi:10.6342/NTU201901077

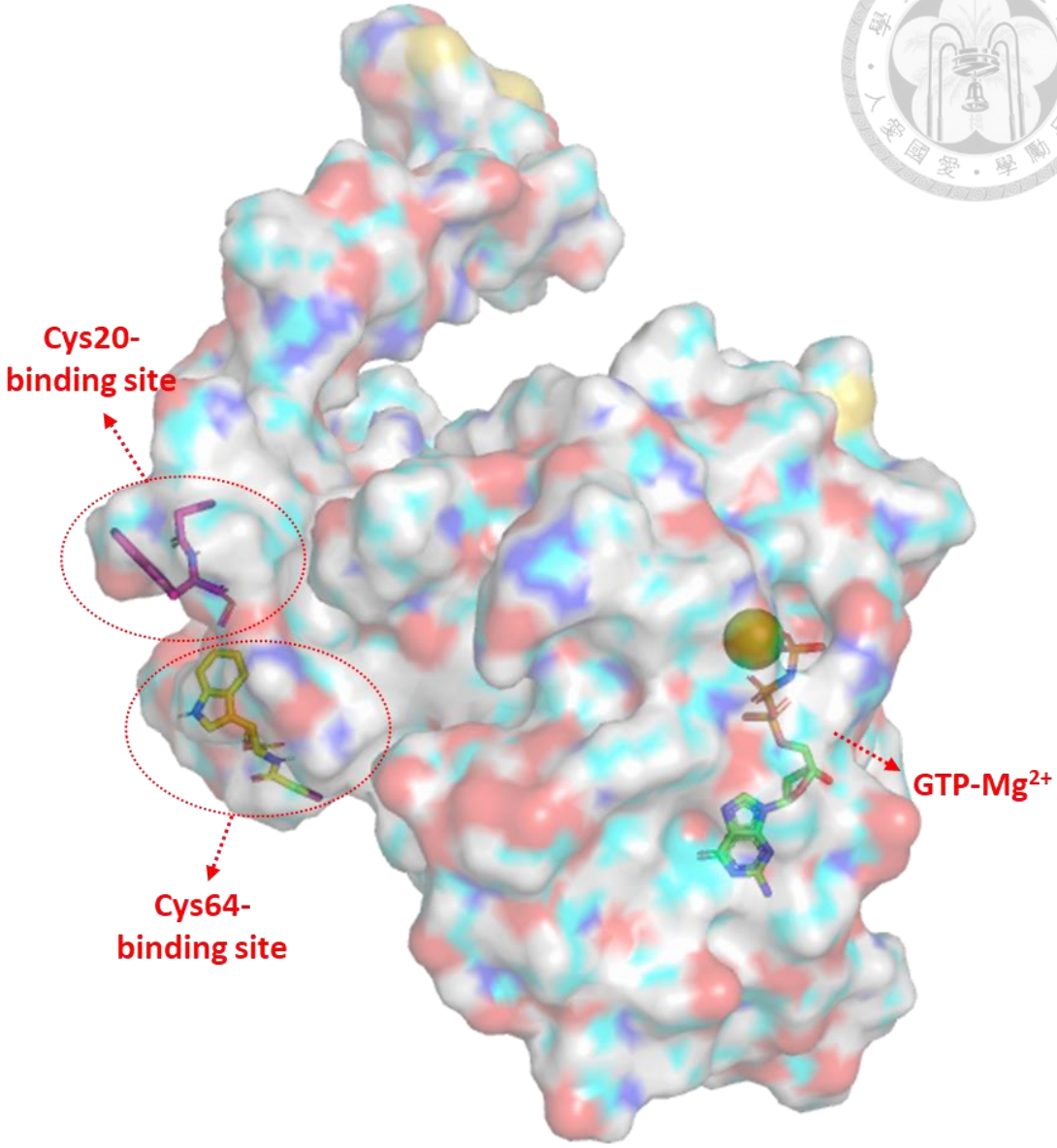

Figure 10. Molecular docking of I-Trp in human Rab5c. The I-Trp binding sites (Cys20 and Cys64) and the active site with the ligand (GTP-Mg^{2+} bound) are shown.

doi:10.6342/NTU201901077

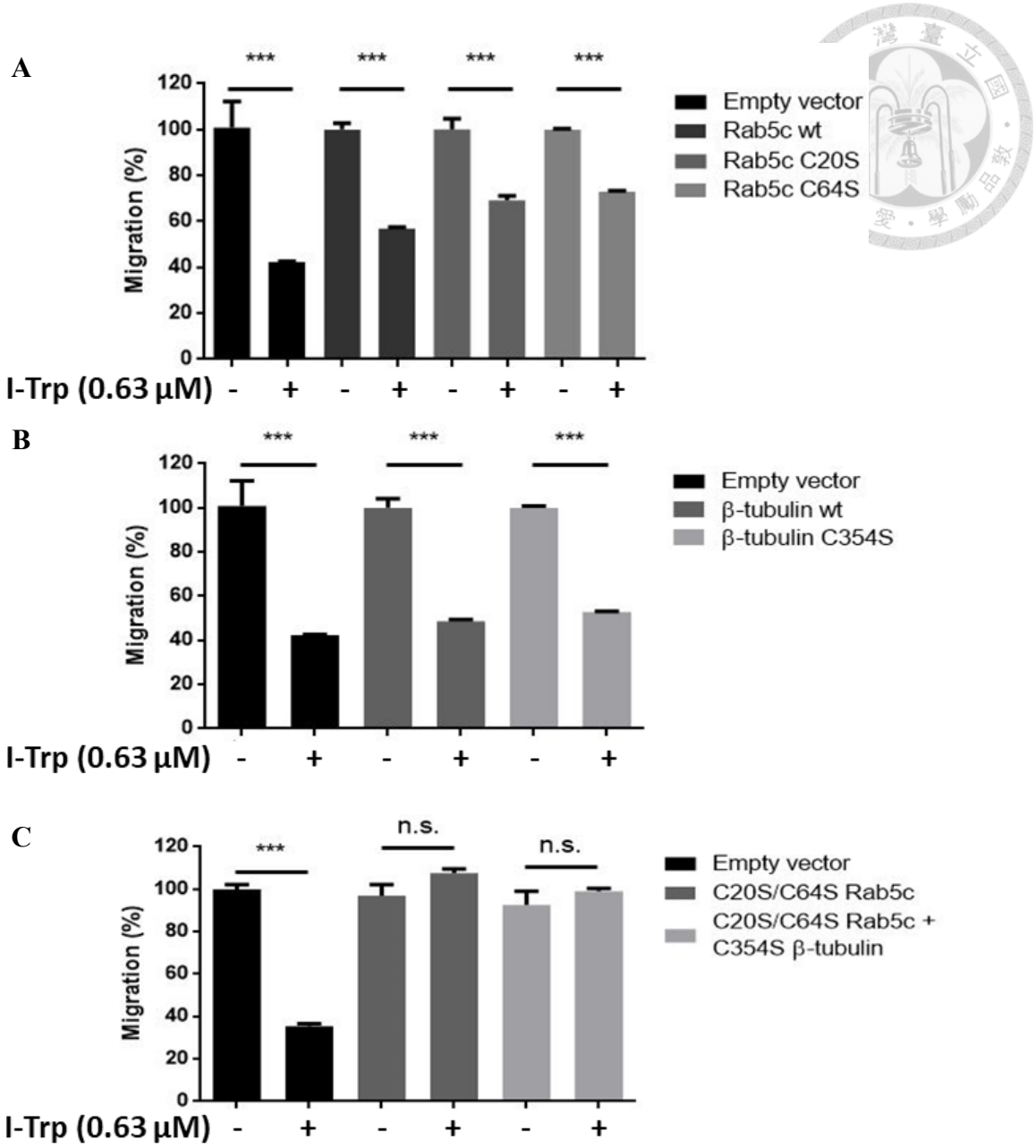

Figure 11. Validation of alkylation at Cys residues in MDA-MB-231 by wound healing assay. (A) MDA-MB-231 expressing either C20S or C64S Rab5c showed less susceptibility to I-Trp treatment. (B) The expression of C354S β-tubulin in MDA-MB-231 resulted in only modest recovery of migratory ability. (C) Double mutants of Rab5c expressed in MDA-MB-231 led to full recovery of MDA-MB-231 migration. Statistical testing was performed by using the unpaired two-sided Student's *t* test; ***P<0.001 versus untreated group, n.s. denotes no statistical significance.

doi:10.6342/NTU201901077

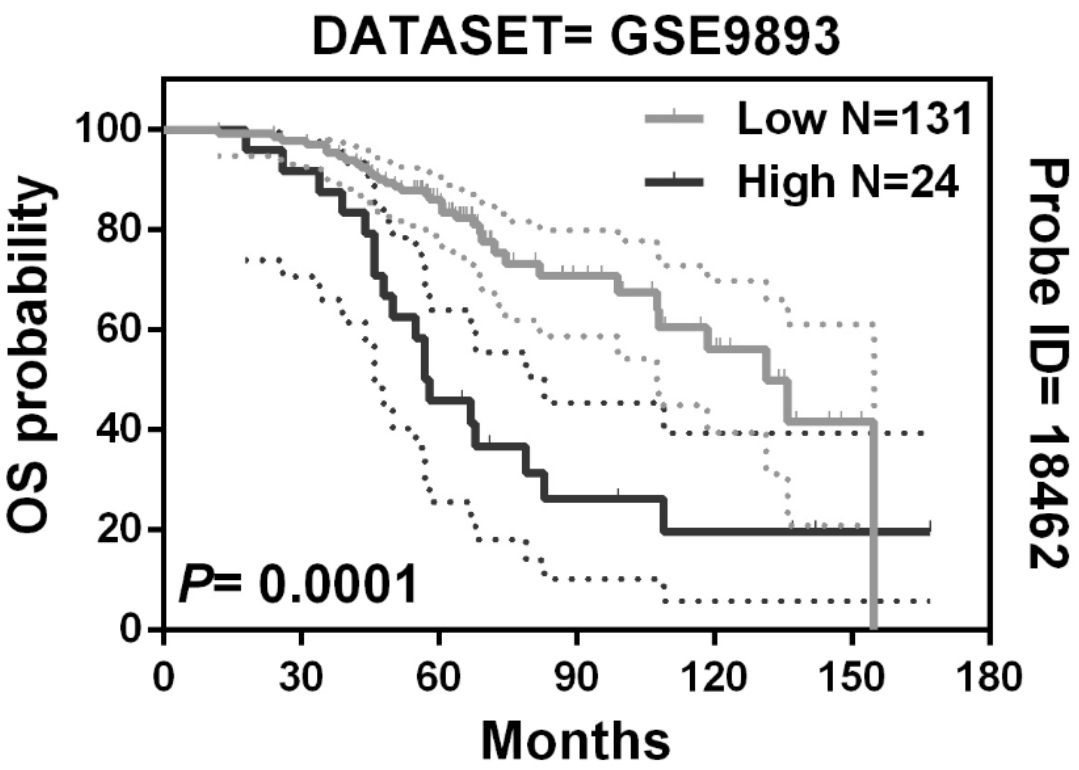

Figure 12. Upregulation of Rab5c is associated with poor patient survival. High versus low Rab5c protein expression was associated with poorer patient survival based on Kaplan–Meier analyses of breast cancer. *P* value was determined by log-rank test. The N value indicates the number of patients.

doi:10.6342/NTU201901077

Reference

1 Bray, F. *et al.* Global cancer statistics 2018: GLOBOCAN estimates of incidence and mortality worldwide for 36 cancers in 185 countries. *CA Cancer J. Clin.* **68**, 394-424, doi:10.3322/caac.21492 (2018).

2 Howlader, N. *et al. SEER Cancer Statistics Review*, retrieved from https://seer.cancer.gov/csr/1975_2014/ (2017).

3 Gibson, R. J. & Keefe, D. M. Cancer chemotherapy-induced diarrhoea and constipation: mechanisms of damage and prevention strategies. *Support. Care Cancer* **14**, 890-900, doi:10.1007/s00520-006-0040-y (2006).

4 Chadha, V. & Shenoi, S. D. Hair loss in cancer chemotherapeutic patients. *Indian J. Dermatol. Venereol. Leprol.* **69**, 131-132 (2003).

5 Can, G., Demir, M., Erol, O. & Aydiner, A. A comparison of men and women's experiences of chemotherapy-induced alopecia. *Eur. J. Oncol. Nurs.* **17**, 255-260, doi:10.1016/j.ejon.2012.06.003 (2013).

6 Brydoy, M., Fossa, S. D., Dahl, O. & Bjoro, T. Gonadal dysfunction and fertility problems in cancer survivors. *Acta Oncol.* **46**, 480-489, doi:10.1080/02841860601166958 (2007).

7 Ito, T. *et al.* Identification of a primary target of thalidomide teratogenicity. *Science* **327**, 1345-1350, doi:10.1126/science.1177319 (2010).

doi:10.6342/NTU201901077

8 Chern, J. *et al.* Affinity-Driven Covalent Modulator of the Glyceraldehyde-3-Phosphate Dehydrogenase (GAPDH) Cascade. *Angew. Chem. Int. Ed. Engl.* **57**, 7040-7045, doi:10.1002/anie.201801618 (2018).

9 Boutros, M. & Ahringer, J. The art and design of genetic screens: RNA interference. *Nat. Rev. Genet.* **9**, 554-566, doi:10.1038/nrg2364 (2008).

10 He, Z. *et al.* Predicting drug-target interaction networks based on functional groups and biological features. *PLoS One* **5**, e9603, doi:10.1371/journal.pone.0009603 (2010).

11 Mei, J. P., Kwoh, C. K., Yang, P., Li, X. L. & Zheng, J. Drug-target interaction prediction by learning from local information and neighbors. *Bioinformatics* **29**, 238-245, doi:10.1093/bioinformatics/bts670 (2013).

12 Stenmark, H. Rab GTPases as coordinators of vesicle traffic. *Nat. Rev. Mol. Cell Biol.* **10**, 513-525, doi:10.1038/nrm2728 (2009).

13 Mendoza, P. *et al.* Rab5 activation promotes focal adhesion disassembly, migration and invasiveness in tumor cells. *J. Cell Sci.* **126**, 3835-3847, doi:10.1242/jcs.119727 (2013).

14 Wehrle-Haller, B. Structure and function of focal adhesions. *Curr. Opin. Cell Biol.* **24**, 116-124, doi:10.1016/j.ceb.2011.11.001 (2012).

15 Lin, Y. F., Tsai, W. P., Liu, H. G. & Liang, P. H. Intracellular beta-

doi:10.6342/NTU201901077

tubulin/chaperonin containing TCP1-beta complex serves as a novel chemotherapeutic target against drug-resistant tumors. *Cancer Res.* **69**, 6879-6888, doi:10.1158/0008-5472.CAN-08-4700 (2009).

16 Lin, Y. F., Lee, Y. F. & Liang, P. H. Targeting beta-tubulin:CCT-beta complexes incurs Hsp90- and VCP-related protein degradation and induces ER stress-associated apoptosis by triggering capacitative Ca2+ entry, mitochondrial perturbation and caspase overactivation. *Cell Death Dis.* **3**, e434, doi:10.1038/cddis.2012.173 (2012).

17 Liu, Y. J., Kumar, V., Lin, Y. F. & Liang, P. H. Disrupting CCT-β : β-tubulin selectively kills CCT-β overexpressed cancer cells through MAPKs activation. *Cell Death Dis.* **8**, e3052, doi:10.1038/cddis.2017.425 (2017).

18 Liang, P. H., Wang, H. M. & Shih, Y. P. Expression vectors for producing tag-cleavable fusion proteins in multiple expression systems. (2009).

19 Friedl, P. & Wolf, K. Tumour-cell invasion and migration: diversity and escape mechanisms. *Nat. Rev. Cancer* **3**, 362-374, doi:10.1038/nrc1075 (2003).

20 Chen, P. I. *et al.* Rab5 isoforms orchestrate a "division of labor" in the endocytic network; Rab5C modulates Rac-mediated cell motility. *PLoS One* **9**, e90384, doi:10.1371/journal.pone.0090384 (2014).

21 Onodera, Y. *et al.* Rab5c promotes AMAP1-PRKD2 complex formation to

doi:10.6342/NTU201901077

enhance beta1 integrin recycling in EGF-induced cancer invasion. *J. Cell Biol.* **197**, 983-996, doi:10.1083/jcb.201201065 (2012).

22 Torres, V. A. *et al.* Rab5 mediates caspase-8-promoted cell motility and metastasis. *Mol. Biol. Cell* **21**, 369-376, doi:10.1091/mbc.E09-09-0769 (2010).

23 Pellinen, T. *et al.* Small GTPase Rab21 regulates cell adhesion and controls endosomal traffic of beta1-integrins. *J. Cell Biol.* **173**, 767-780, doi:10.1083/jcb.200509019 (2006).

24 Steeg, P. S. Perspective: The right trials. *Nature* **485**, S58-59, doi:10.1038/485S58a (2012).

25 Conner, S. D. & Schmid, S. L. Regulated portals of entry into the cell. *Nature* **422**, 37-44, doi:10.1038/nature01451 (2003).

26 Ivaska, J. & Heino, J. Cooperation between integrins and growth factor receptors in signaling and endocytosis. *Annu. Rev. Cell. Dev. Biol.* **27**, 291-320, doi:10.1146/annurev-cellbio-092910-154017 (2011).

27 Caswell, P. T. & Norman, J. C. Integrin trafficking and the control of cell migration. *Traffic* **7**, 14-21, doi:10.1111/j.1600-0854.2005.00362.x (2006).

28 Qualmann, B. & Kessels, M. M. Endocytosis and the cytoskeleton. *Int. Rev. Cytol.* **220**, 93-144 (2002).

29 Bucci, C. *et al.* The Small Gtpase Rab5 Functions as a Regulatory Factor in the

doi:10.6342/NTU201901077

Early Endocytic Pathway. *Cell* **70**, 715-728, doi:10.1016/0092-8674(92)90306-W (1992).

30 Simonsen, A. *et al.* EEA1 links PI(3)K function to Rab5 regulation of endosome fusion. *Nature* **394**, 494-498, doi:10.1038/28879 (1998).

31 Nielsen, E., Severin, F., Backer, J. M., Hyman, A. A. & Zerial, M. Rab5 regulates motility of early endosomes on microtubules. *Nat. Cell Biol.* **1**, 376-382, doi:10.1038/14075 (1999).

32 Diaz, J. *et al.* Rab5 is required in metastatic cancer cells for Caveolin-1-enhanced Rac1 activation, migration and invasion. *J. Cell Sci.* **127**, 2401-2406, doi:10.1242/jcs.141689 (2014).

33 Liu, S. S., Chen, X. M., Zheng, H. X., Shi, S. L. & Li, Y. Knockdown of Rab5a expression decreases cancer cell motility and invasion through integrin-mediated signaling pathway. *J. Biomed. Sci.* **18**, 58, doi:10.1186/1423-0127-18-58 (2011).

doi:10.6342/NTU201901077